ELSEVIER

International Journal of Heat and Fluid Flow 22 (2001) 213–219

International Journal of HEAT AND FLUID FLOW

www.elsevier.com/locate/ijhff

A study on spanwise heat transfer in a turbulent channel flow – eduction of coherent structures by a conditional sampling technique

K. Matsubara [a,*], M. Kobayashi [a], T. Sakai [b], H. Suto [b]

[a] *Department of Mechanical and Production Engineering, Faculty of Engineering, Niigata University, Ikarashi 2-nocho 8050, Niigata 950-2181, Japan*
[b] *Graduate School of Science and Technology, Niigata University, Ikarashi 2-nocho 8050, Niigata, Japan*

Abstract

Coherent structures of temperature fields in the near-wall turbulence ($y^+ < 60$) were educed by a conditional sampling technique from the DNS data. Treated situation is the fully developed turbulent channel flow for two kinds of temperature fields: (a) the uniform heat flux assigned on two walls of the channel (UHF) and (b) the constant spanwise mean temperature gradient imposed on the flow over the whole channel width (STG). Following conclusions are obtained. (1) Flow and temperature fields around the quasi-streamwise vortex are roughly uniform in the streamwise direction. (2) Temperature distribution in/around the vortex for UHF and that for STG are similar in shape with azimuthal phase difference of about 90°. (3) Mechanisms for destruction of turbulent heat flux are similar between UHF case and STG case.

1. Introduction

Turbulent heat transfer from the wall is one of the basic subjects in heat transfer engineering. Detailed features of it have been keenly studied especially for the case where thermal boundary condition on the wall is uniform and net spanwise transfer of heat does not occur. However, in many practical applications, e.g., gas turbine blades, heat exchangers and boilers, and in heat transfer problems, e.g., electronics cooling and atmospheric heat diffusion, thermal boundary condition is usually non-uniformly distributed and three-dimensionality of temperature field exists.

Therefore, spanwise heat transfer in turbulent boundary layer was examined both experimentally and numerically and fundamental aspects of its statistical feature were reported (Black and Sparrow, 1967; Quarmby and Quirk, 1972; Maekawa et al., 1991; Matsubara et al., 1997, 1998). For example, the eddy diffusivity ratio $\varepsilon_{hz}/\varepsilon_{hy}$, the ratio between spanwise and wall-normal components of eddy diffusivity of heat, is almost uniform in the fully turbulent region but it rapidly increases when approaching the wall. However, there still remain many unknown points in mechanisms of spanwise heat transfer near the wall. The present study is an extension of the previous DNS for statistical analysis of spanwise heat transfer (Matsubara et al., 1997, 1998) and aims to reveal its coherent structure. For this purpose, conditional sampling technique was applied to the DNS data of fully developed turbulent channel flow for two kinds of temperature fields: (a) the case of uniformly heated walls and (b) the case of spanwise mean temperature non-uniformity imposed on the fluid. In the discussion, special attention is paid to the roles of the quasi-streamwise vortex which was found to play a key role in transport phenomena in the near-wall region ($y^+ < 60$) (Brooke and Hanratty, 1993; Miyake et al., 1995; Jeong et al., 1997). It has been already examined how the near-wall phenomena are controlled by the quasi-streamwise vortex in the case of uniformly heated walls, and therefore the main subject in this paper is to obtain new insight into heat transfer mechanisms in the case of spanwise temperature gradient. Discussions on the case of uniformly heated walls are necessary because two cases of temperature fields are compared with each other for a better understanding of the spanwise heat transfer case.

2. Numerical method

The computational domain and coordinate system are shown in Fig. 1. The streamwise, wall-normal and spanwise coordinates are denoted by x, y and z. Simulation is made for fully developed turbulent channel flow for two kinds of temperature fields. One is the usual case of two-dimensional heat transfer from the wall where the wall is uniformly heated by constant heat flux (UHF). In this case, turbulent transfer of heat occurs in x and y directions, and net spanwise transfer of heat does not appear. Another is the simple case of spanwise heat transfer in the wall turbulence where the spanwise mean temperature gradient prevails over the channel width and the turbulent heat flux has only spanwise component (STG). The

* Corresponding author. Tel.: +81-25-262-6715; fax: +81-25-262-6715.
E-mail address: matsu@tmtherm.eng.niigata-u.ac.jp (K. Matsubara).

0142-727X/01/$ - see front matter
PII: S0142-727X(01)00082-0

Notation

C_P	specific heat at constant pressure (J/Kg K)
L_x, L_z	computational domain size in x and z directions (m)
P	pressure (Pa)
p	pressure fluctuation (Pa)
Pr	Prandtl number $= \nu/\alpha$
q_W	wall heat flux in UHF (W/m^2)
Re	Reynolds number $= U_\tau\delta/\nu$
S_{ij}	symmetric part of velocity gradient tensor (1/s)
T	temperature (K)
T_τ	friction temperature in UHF $= q_W/(\rho C_P U_\tau)$ (K)
T_{STG}	temperature scale in STG $= -\alpha(\partial T/\partial z)/U_\tau$ (K)
t	time normalized by δ/U_τ
U	velocity component in the x direction (m/s)
U_τ	friction velocity (m/s)
U_i	velocity component in the ith direction (m/s)
u, v, w	velocity fluctuation in x, y and z directions (m/s)
u_i	ith component of velocity fluctuation (m/s)
x, y, z	streamwise, wall-normal and spanwise coordinates normalized by δ (m)
x_i	coordinate normalized by δ in the ith direction; x_1, x_2 and x_3 denote x, y and z, respectively (m)
α	thermal diffusivity (m^2/s)
Δt	time step (s)
$\Delta x, \Delta y, \Delta z$	grid spacing in x, y and z directions (m)
δ	channel half-width (m)
δ_{ij}	Kronecker's delta
$\varepsilon_{hy}, \varepsilon_{hz}$	eddy diffusivity of heat in y and z directions (m^2/s)
θ	temperature fluctuation (K)
λ	second invariant of the velocity gradient tensor (m^2/s^2)
ν	kinematic viscosity (m^2/s)
ρ	density (kg/m^3)
φ	physical quantity
Ω_{ij}	anti-symmetric part of the velocity gradient tensor (1/s)
ω_x	streamwise vorticity (1/s)
$^+$	normalized by U_τ, ν and T_τ
*	normalized by T_{STG}
$_{rms}$	fluctuation intensity
$\langle\ \rangle$	conditional mean
$\bar{}$	time mean

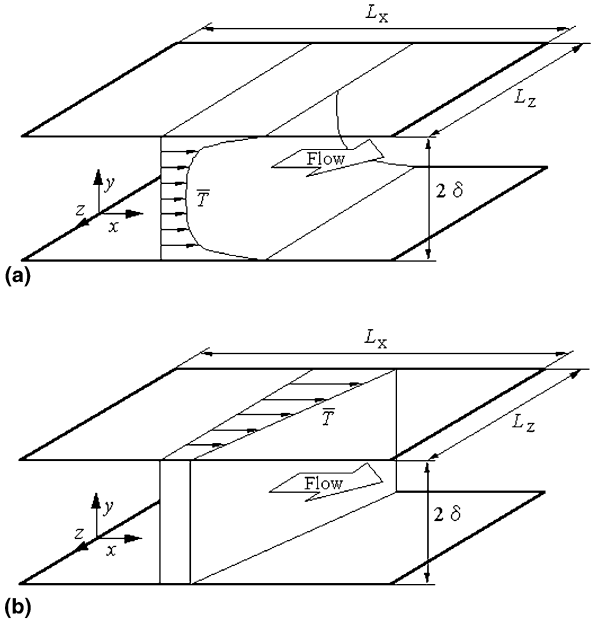

Fig. 1. Computational domain and coordinate system: (a) uniform heat flux on the wall; (b) spanwise temperature gradient.

latter is somewhat artificial but provides a good arena for discussion of spanwise heat transfer because of its simplicity (Matsubara et al., 1997, 1998).

Basic equations for the flow field are the continuity and Navier–Stokes equations:

$$\frac{\partial U_i^+}{\partial x_i} = 0, \tag{1}$$

$$\frac{\partial U_i^+}{\partial t} + U_j^+\frac{\partial U_i^+}{\partial x_j} = -\frac{\partial P^+}{\partial x_i} + \frac{1}{Re}\frac{\partial^2 U_i^+}{\partial x_j^2} + \delta_{1i}, \tag{2}$$

where δ_{1i} corresponds to the mean pressure gradient driving the working fluid. The dimensionless temperature for UHF and that for STG are defined as

$$\Theta^+ = (T - T_W)/T_\tau \quad \text{for UHF}, \tag{3}$$

$$\Theta^* = (T - T_W)/T_{STG} \quad \text{for STG}, \tag{4}$$

where T_τ and T_{STG} are the friction temperature for UHF and reference temperature for STG (see Chapter 2). Energy equation used for UHF and that for STG are then written as

$$\frac{\partial\Theta^+}{\partial t} + U_j^+\frac{\partial\Theta^+}{\partial x_j} = \frac{1}{RePr}\frac{\partial^2\Theta^+}{\partial x_j^2} - \frac{U_1^+}{U_m^+} \quad \text{for UHF}, \tag{5}$$

$$\frac{\partial\Theta^*}{\partial t} + U_j^+\frac{\partial\Theta^*}{\partial x_j} = \frac{1}{RePr}\frac{\partial^2\Theta^*}{\partial x_j^2} + RePrU_3^+ \quad \text{for STG}. \tag{6}$$

The last term on (5) and that on (6) represent production by streamwise mean temperature gradient, $-U_1^+\partial T_W^+/\partial x_1$, and production by spanwise mean temperature gradient, $-U_3^+\partial T_W^*/\partial x_3$, respectively. Periodicity condition is applied for x and z directions for velocity and temperature fields. The velocity components and temperature fluctuation for two cases are all set to zero on the wall of the channel. Fourth-order central finite difference is applied for the discretization of basic equations. More detailed description of the numerical scheme should be referred in the literatures (Matsubara et al., 1997, 1998). Numerical conditions taken in this paper are listed in Table 1. Reynolds number based on the friction velocity and the channel half-width, Re was set to 150, and the Prandtl number, Pr, to 0.71 (air). Uniform grid mesh is used in x and z directions with non-uniform spacing in the y direction. Under the grid resolution presented in Table 1 the flow field data show good agreement with other DNS results (Kasagi et al., 1992a) obtained by the spectral method, and the computational validity is thus confirmed (Matsubara et al., 1997, 1998).

3. Conditional sampling technique

In order to obtain coherent structures, conditional sampling technique proposed by Jeong et al. (1997) is used with minor change. In the original scheme by Jeong et al. (1997) eigenvalue of the tensor, $S_{ik}S_{kj} + \Omega_{ik}\Omega_{kj}$, was used to detect the

Table 1
Computational conditions

Re	150
Pr	0.71
L_x/δ	7.85
L_z/δ	3.14
Grid points	$64 \times 61 \times 64$
Δx^+	18.4
Δy^+	1.03–9.51
Δz^+	7.36
Δt^+	0.06

vortex, while in the present study second invariant of the deformation tensor, λ, is used for this purpose. However, it was found that vortical structures educed by both detectors are almost identical. In Fig. 2, iso-surface of λ for the near-wall region ($y^+ < 60$) is presented. Vortical structures are elongated in the streamwise direction, and their streamwise extents are roughly 200 wall units.

Conditional sampling scheme (Jeong et al., 1997) used here consists of three procedures.

1. To find the center-axis of the quasi-streamwise vortex, local maxima of $-\lambda$ in the y–z plane were first detected in the near-wall region $10 < y^+ < 40$ under condition that $-\lambda > -(\lambda - \widetilde{\lambda})_{\mathrm{rms}}$ and that $\omega_x > 0$ (or $\omega_x < 0$). Due to the latter condition, vortical structures having the same sense of streamwise rotation are captured.
2. When the local maxima are continuously distributed in the streamwise direction over 150 wall units, the mid-point for the streamwise extent of this distribution (corresponding to center-axis of vortical structure) is taken as a reference point of averaging.
3. Instantaneous flow and thermal fields are averaged putting the origin of x and z on the reference points found in (2).

Averaged structures obtained by the above procedure with positive and negative senses of rotation are called SP and SN, respectively. In the present study, 50 sets of instantaneous data are kept at every 500 time step for conditional sampling, and 177 and 180 vortical structures for SP and SN are detected.

Using the conditionally averaged variable, instantaneous velocity, U_i, is decomposed as

$$U_i = \langle U_i \rangle + u_i', \tag{7}$$

where $\langle U_i \rangle$ is the conditional mean of U_i or coherent part of it, and u_i' denotes incoherent part of U_i. Decomposition can also be made for velocity fluctuation, u_i, meaning deviation from the usual mean velocity, $\overline{U}_i$,

$$u_i = \langle u_i \rangle + u_i'. \tag{8}$$

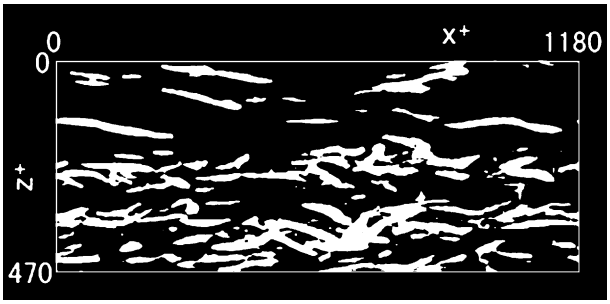

Fig. 2. Second invariant of deformation tensor in the range of $0 < y^+ < 60$, white blobs indicate $-\lambda^+ > 0.02$.

Eq. (8) and similar expression for temperature fluctuation yield

$$\langle u_i \theta \rangle = \langle u_i \rangle \langle \theta \rangle + \langle u_i' \theta' \rangle. \tag{9}$$

As seen above, conditionally averaged correlation between u_i and θ, $\langle u_i \theta \rangle$ includes the term $\langle u_i' \theta' \rangle$ which appears due to incoherent motion and smears structures educed by conditional sampling. To eliminate this smearing, not $\langle u_i \theta \rangle$ but $\langle u_i \rangle \langle \theta \rangle$ is used in the discussion of apparent heat flux caused by coherent structure, i.e., coherent heat flux (see Section 4.3). Similar discussion can be made for second invariant of deformation tensor, $\lambda (= \partial u_i/\partial x_j \cdot \partial u_j/\partial x_i)$. Conditionally averaged value of λ,

$$\langle \lambda(\partial u_i/\partial x_j) \rangle = \langle \partial u_i/\partial x_j \cdot \partial u_j/\partial x_i \rangle, \tag{10}$$

and λ of conditionally averaged deformation tensor,

$$\lambda(\partial \langle u_i \rangle/\partial x_j) = \partial \langle u_i \rangle/\partial x_j \cdot \partial \langle u_j \rangle/\partial x_i, \tag{11}$$

are related by the relation,

$$\langle \lambda(\partial u_i/\partial x_j) \rangle = \lambda(\partial \langle u_i \rangle/\partial x_j) + \langle \partial u_i'/\partial x_j \cdot \partial u_i'/\partial x_j \rangle. \tag{12}$$

Since the former (10) is affected by incoherent part of u, the latter (11) is used for the discussion in this section. The value of (11) is shown for SP and SN in Figs. 3 and 4, respectively.

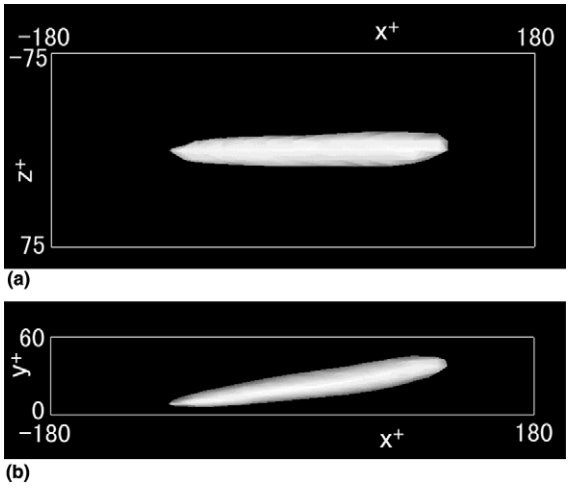

Fig. 3. $\lambda(\partial \langle u_i \rangle/\partial x_j)$ for SP, white blob indicates $-\lambda^+ > 0.004$: (a) top view; (b) side view.

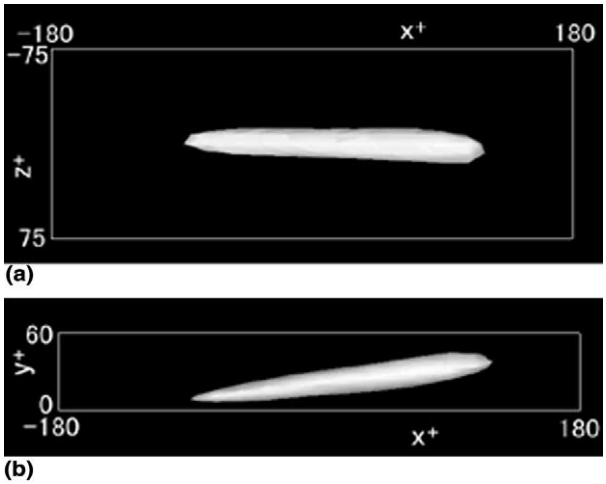

Fig. 4. $\lambda(\partial \langle u_i \rangle/\partial x_j)$ for SN, white blob indicates $-\lambda^+ > 0.004$: (a) top view; (b) side view.

Both SP and SN are presented in order to check convergence of averaged quantity. As seen in Figs. 3 and 4, quasi-streamwise structure tilt in the x–z plane, and direction of the tilt for SP and SN are inverted. The streamwise-structure is inclined in the x–y plane and their inclination angles are roughly the same. Good symmetry between SP and SN suggests that highly converged values are obtained by conditional sampling. Since SP and SN are symmetrical counterparts as suggested in Figs. 3 and 4, attention is paid only to SP in the following discussion.

4. Results and discussion

4.1. Flow field

Jeong et al. (1997) gave a detailed description of the flow field data obtained by conditional sampling. However, coherent structure of the flow field is briefly outlined here in order to prepare for the discussion of temperature field. Fig. 5 shows conditionally averaged velocity field around the quasi-streamwise vortex having positive sense of streamwise rotation (SP). Three flames in Fig. 5 are sampled at $x = 0, z = 0$ and $y^+ = 20$, and each flame includes the contours for streamwise component of fluctuation velocity, $\langle u \rangle$ and vectors of secondary flow (i.e. transverse components). Shaded parts in the figure indicate positive value of $\langle u \rangle$, and three numbers C1, C2, C3 written below the flame as (C1, C2, C3) are contour spacing, minimum contour and maximum contour, respectively. Note that similar expressions are used in the following figures. For simpler description, conditionally averaged value of velocity fluctuation, $\langle u \rangle$, is called merely velocity fluctuation in parts of the following discussion.

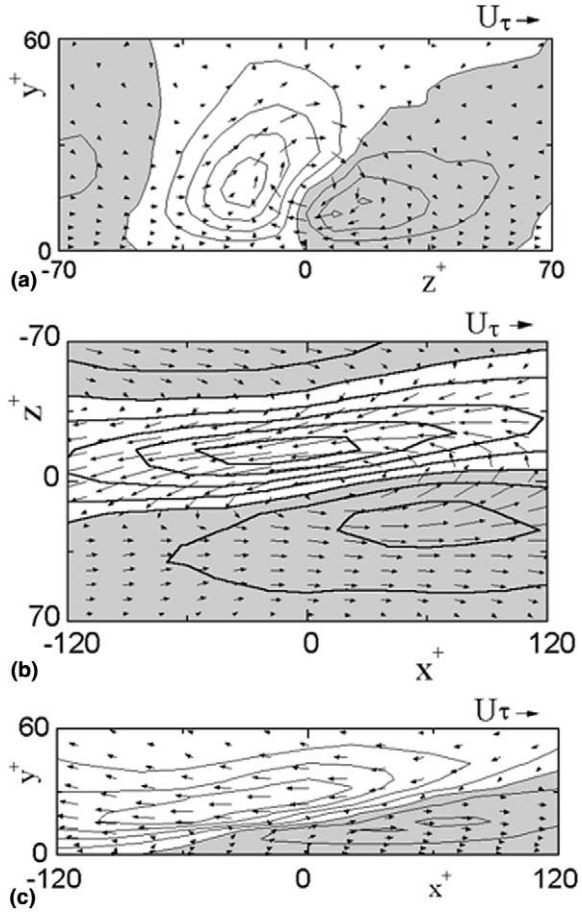

Fig. 5. Contours of $\langle u^+ \rangle$ for SP: (a) $x = 0$, contour levels = (contour spacing, minimum, maximum) = (0.6, −2.4, 1.8); (b) $y^+ = 20$, contour levels = (0.6, −2.4, 1.2); (c) $z = 0$, contour levels = (0.32, −1.3, 0.64).

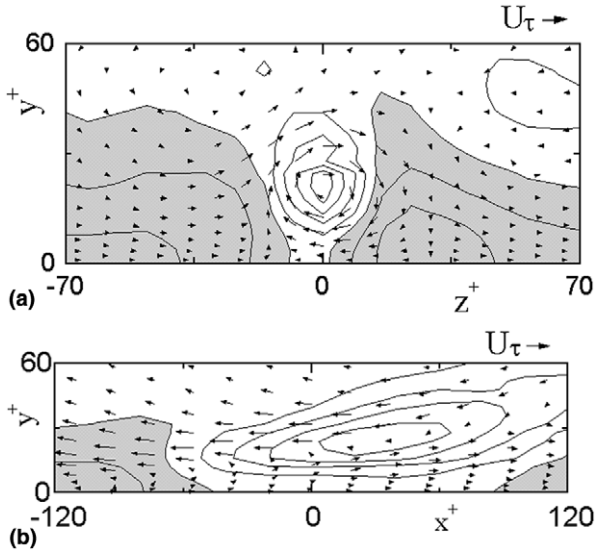

Fig. 6. Contours of $\langle p^+ \rangle$ for SP: (a) $x = 0$, contour levels = (0.28, −1.1, 0.56); (b) $z = 0$, contour levels = (0.34, −1.4, 0.68).

As seen in Fig. 5(b) and (c), $\langle u \rangle$ changes more slowly in the streamwise direction than in other directions, and velocity distribution is roughly uniform in the streamwise direction. In Fig. 5(a), upward and downward flow motions are observed around the vortex, and they cause streamwise velocity fluctuation, $\langle u \rangle < 0$ and $\langle u \rangle > 0$, due to the presence of the background shear. Interface between fast ($\langle u \rangle > 0$) and slow ($\langle u \rangle < 0$) fluids is slightly inclined to the wall-normal coordinate since excess momentum fluid is transported by the convective effect of the vortex. This results in the inverted gradient of the velocity fluctuation so that mean streamwise velocity and its fluctuation part have opposite gradients in the wall-normal direction. As discussed later, similar phenomenon seen in the temperature field is one of the reasons for destructing turbulent heat flux.

The pressure field is shown in Fig. 6. Low-pressure fluid core exists inside the vortical structure, and balances with the centrifugal force generated by the rotation. As seen later, presence of this low-pressure core is another factor for the destruction of turbulent heat flux.

4.2. Temperature field

Conditionally averaged temperature $\langle \theta \rangle$ for UHF and that for STG are shown in Figs. 7 and 8, respectively. In parts of the following, $\langle \theta \rangle$ is merely temperature fluctuation to simplify the description. Temperature distributions around the vortex for both cases are nearly uniform in the streamwise direction. In the case of UHF, temperature distribution is almost identical to the distribution of the streamwise velocity, suggesting a similarity between flow and temperature fields. In UHF, fluctuation temperature $\langle \theta \rangle$ is caused by the wall-normal velocity component, and it is large at right- and left-halves of the vortex. In this case, near the center-axis of the vortex, wall-normal gradient of fluctuation temperature becomes positive, while negative gradient is imposed on the mean temperature.

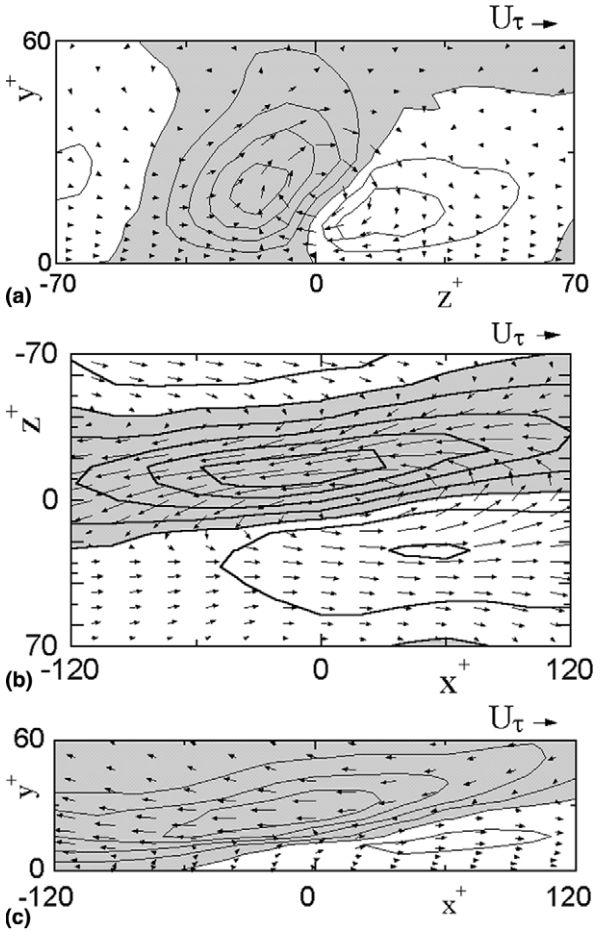

Fig. 7. Contours of $\langle\theta^+\rangle$ for SP in UHF: (a) $x = 0$, contour levels = (0.55, −1.1, 2.2); (b) $y^+ = 20$, contour levels = (0.55, −1.1, 2.2); (c) $z = 0$, contour levels = (0.34, −0.68, 1.4).

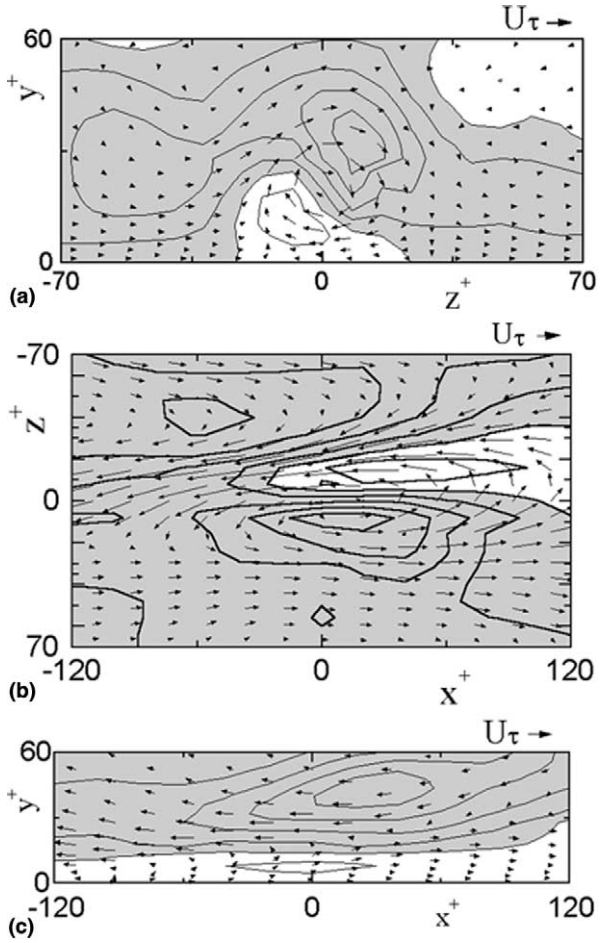

Fig. 8. Contours of $\langle\theta^*\rangle$ for SP in STG: (a) $x = 0$, contour levels = (3.0, −3.0, 12); (b) $y^+ = 20$, contour levels = (2.2, −2.2, 8.8); (c) $z = 0$, contour levels = (2.8, −2.8, 11).

Thus, inverted gradient of temperature fluctuation occurs in wall-normal direction in the UHF case. In the case of STG, temperature fluctuation takes high value at upper- and lower-halves of the vortex due to spanwise velocity component and inverted gradient of temperature fluctuation appear in the spanwise direction. Therefore, temperature distribution in STG and that in UHF are roughly similar in shape, but phase difference of nearly 90° exists between these.

4.3. Convective heat flux due to vortical flow motion

In this section, discussed is the convective heat flux $\langle u_i\rangle\langle\theta\rangle$ which corresponds to heat flux due to convective effect of vortical flow motion. The use of $\langle u_i\rangle\langle\theta\rangle$ instead of $\langle u_i\theta\rangle$ is based on the same reason as described in the discussion of second invariant of deformation tensor (see Chapter 4). In this study $\langle u\rangle\langle\theta\rangle$ and $\langle v\rangle\langle\theta\rangle$ for UHF and $\langle w\rangle\langle\theta\rangle$ for STG have non-zero values, and they are plotted in Fig. 9. In Fig. 9(a), streamwise component of coherent heat flux, $\langle u\rangle\langle\theta\rangle$, is large at right- and left-sides of vortex center due to velocity fluctuation in y, and it takes negative value almost over the whole width of the plane presented in the figure. The latter suggests that in the case of UHF correlation between u and θ is very high near the wall (Kasagi et al., 1992b).

Wall-normal heat flux, $\langle v\rangle\langle\theta\rangle$, for UHF and the spanwise component, $\langle w\rangle\langle\theta\rangle$, for STG represent the convective heat transport parallel to the mean temperature gradient. Because of similarity between temperature distribution around the vortex for UHF and that for STG, distribution of $\langle v\rangle\langle\theta\rangle$ and that of $\langle w\rangle\langle\theta\rangle$ are again similar in shape with azimuthal phase difference of 90°. The similarity in coherent structures should be background for the statistical similarity such that correlation coefficient between v and θ for UHF and that between w and θ for STG are nearly equal over the channel width excluding the channel central part ($100 < y^+ < 150$) where $\langle v\rangle\langle\theta\rangle$ vanishes due to the flow symmetry but the value of $\langle w\rangle\langle\theta\rangle$ remains.

4.4. Production and destruction of turbulent heat flux

Examination is given to two major processes in the turbulent heat flux transport, production and destruction (Matsubara et al., 1997, 1998; Kasagi et al., 1992b). In the situation taken here, they are defined as listed in Table 2. In Fig. 10, for UHF presented are conditionally averaged quantities

$$-\langle u\rangle\langle v\rangle\partial\overline{T}/\partial y - \langle v\rangle\langle\theta\rangle \mathrm{d}\overline{U}/\mathrm{d}y, \tag{13}$$

$$\langle p\rangle \mathrm{d}\langle\theta\rangle/\mathrm{d}x. \tag{14}$$

The former and the latter correspond to production and destruction, respectively, of streamwise turbulent heat flux for the UHF case, where production by streamwise temperature gradient $\langle u\rangle^2\partial\overline{T}/\partial x$ was confirmed to be very small and thus

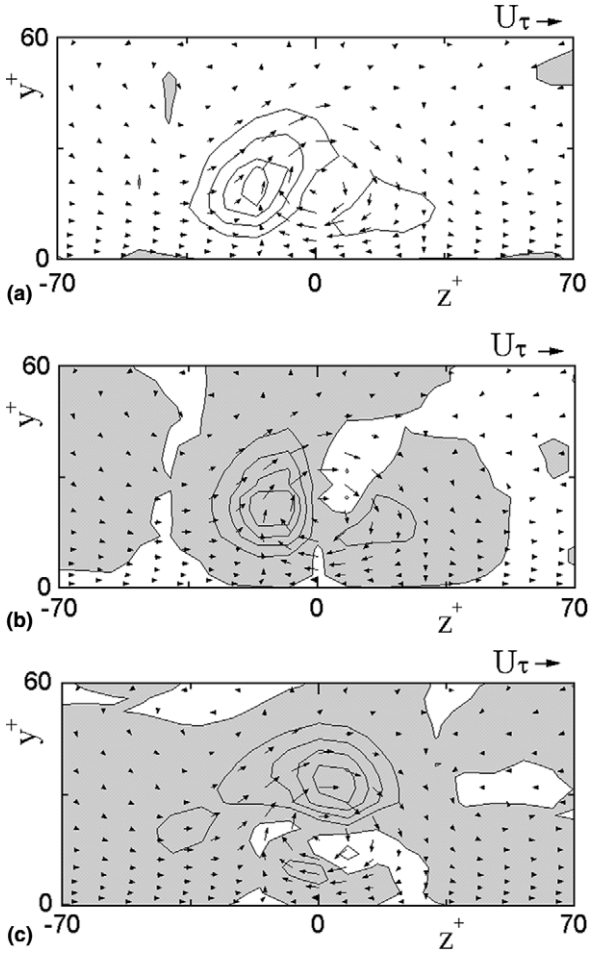

Fig. 9. Coherent heat flux for SP at $x = 0$: (a) $\langle u^+\rangle\langle\theta^+\rangle$ in UHF, contour levels = (1.8, 7.0, 0.0); (b) $\langle v^+\rangle\langle\theta^+\rangle$ in UHF, contour levels = (0.36, 0.0, 1.4); (c) $\langle w^+\rangle\langle\theta^*\rangle$ in STG, contour levels = (2.6, −2.6, 10).

Table 2
Production and destruction of turbulent heat flux

Turbulent heat flux	Production	Destruction
$\overline{u\theta} < 0$	$-\overline{uv}\frac{\partial\overline{T}}{\partial y} - \overline{u^2}\frac{\partial\overline{T}}{\partial x} - \overline{v\theta}\frac{\partial\overline{U}}{\partial y} < 0$	$\overline{p\frac{\partial\theta}{\partial x}} > 0$
$\overline{v\theta} > 0$	$-\overline{uv}\frac{\partial\overline{T}}{\partial x} - \overline{v^2}\frac{\partial\overline{T}}{\partial y} > 0$	$\overline{p\frac{\partial\theta}{\partial y}} < 0$
$\overline{w\theta} > 0$	$-\overline{w^2}\frac{\partial\overline{T}}{\partial z} > 0$	$\overline{p\frac{\partial\theta}{\partial z}} < 0$

was omitted from Eq. (13). The comparison between the first and second terms in (13) revealed that these values are almost equal due to the similarity between flow and thermal fields in the UHF case. As seen in Fig. 10, production is conspicuous at right- and left-sides of vortex core where $\langle u\rangle, \langle v\rangle$ and $\langle\theta\rangle$ included in (13) are large, and destruction takes a high positive value near the vortex center. Since production and destruction occur in clearly separated regions, spatial transport effect such as turbulent diffusion or pressure diffusion should have a role in the transport between separated regions. Destruction of heat flux in this case is caused by two factors. The first is the rotating flow motion of the vortex, which induces negative pressure fluctuation ($\langle p\rangle < 0$) within the vortex core. The second is the tilting and inclination of the vortex, which

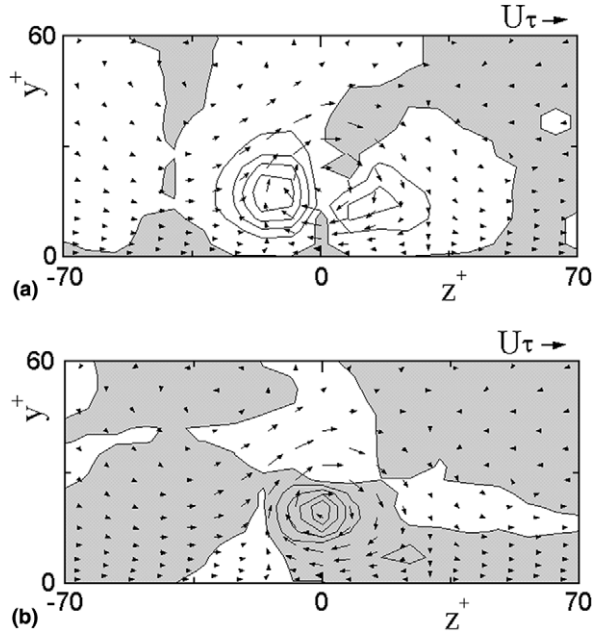

Fig. 10. Production and destruction of coherent streamwise heat flux for SP in UHF at $x = 0$: (a) $-\langle u^+\rangle\langle v^+\rangle\partial\overline{T^+}/\partial y^+ - \langle v^+\rangle\langle\theta^+\rangle\mathrm{d}\overline{U^+}/\mathrm{d}y^+$, contour levels = (0.22, −0.72, 0.0); (b) $\langle p^+\rangle\mathrm{d}\langle\theta^+\rangle/\mathrm{d}x^+$, contour levels = (0.006, 0.0, 0.024).

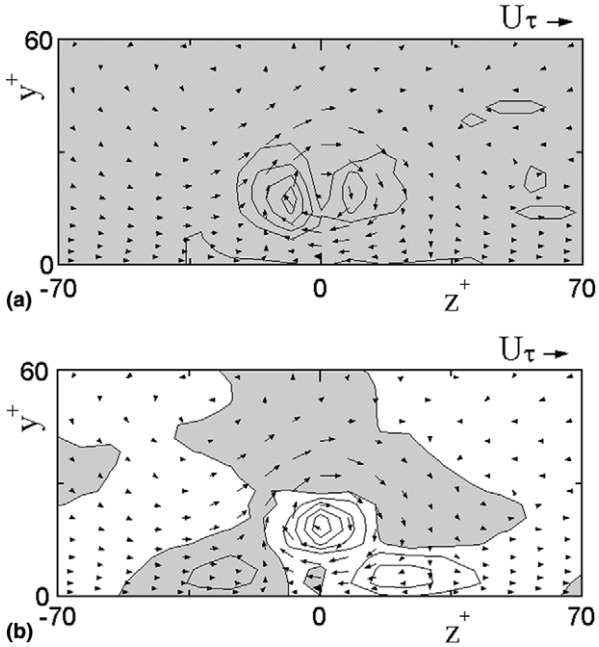

Fig. 11. Production and destruction of coherent wall-normal heat flux for SP in UHF at $x = 0$: (a) $-\langle v^+\rangle^2\partial\overline{T^+}/\partial y^+$, contour levels = (0.036, 0.036, 0.144); (b) $\langle p^+\rangle\partial\langle\theta^+\rangle/\partial y^+$, contour levels = (0.044, −0.18, 0.044).

result in negative gradient of fluctuation temperature ($\partial\langle\theta\rangle/\partial x < 0$).

Conditionally averaged statistics corresponding to production and destruction of wall-normal turbulent heat flux for UHF

$$-\langle v\rangle^2\partial\overline{T}/\partial y, \tag{15}$$

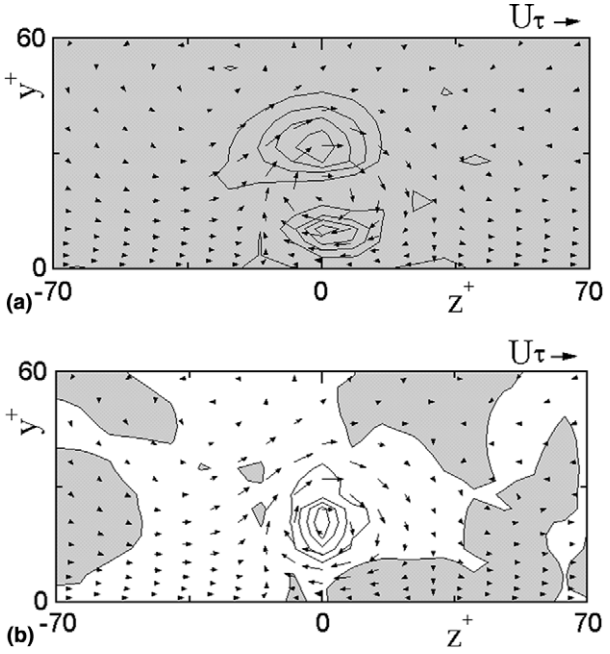

Fig. 12. Production and destruction of coherent spanwise heat flux for SP in STG at $x = 0$: (a) $-\langle w^+\rangle^2 \mathrm{d}\overline{T^*}/\mathrm{d}z^+$, contour levels = (0.18, 0.18, 0.72); (b) $\langle p^+\rangle \partial\langle\theta^*\rangle/\partial z^+$, contour levels = (0.28, −1.1, 0.0).

$$\langle p\rangle \partial\langle\theta\rangle/\partial y \tag{16}$$

are plotted in Fig. 11. In Eq. (15), the term $\langle u\rangle\langle v\rangle\partial\overline{T}/\partial x$ is neglected because it was found to be quite small. In Fig. 12, plotted are the quantities for STG

$$-\langle w\rangle^2 \mathrm{d}\overline{T}/\mathrm{d}z, \tag{17}$$

$$\langle p\rangle \partial\langle\theta\rangle/\partial z, \tag{18}$$

expressing production and destruction of spanwise turbulent heat flux. The values of productions (15) and (17) should be positive due to their definitions, and they are actually positive everywhere in the visualized flame. They take large values at the outer-peripheral of the vortex where velocity fluctuations are also high, and the destructions (16) and (18) are conspicuous at the central part of the vortex. As seen in Figs. 6–8, destruction of wall-normal heat flux and that of spanwise component are based on similar mechanisms. In both, destruction occurs due to the rotating flow motion of the vortex, which results in low pressure within the vortex core and inverted gradient of temperature fluctuation near the center-axis of the vortex.

5. Conclusions

Conditionally averaged structures were obtained from the channel flow DNS data for two kinds of temperature fields: (a) uniform heat flux heating on the wall (UHF), (b) spanwise temperature gradient over the whole channel width (STG). Average was made conditionally upon quasi-streamwise vortex near the wall, and coherent structures of temperature were obtained. Main conclusions are as follows:

1. Conditionally averaged flow field around the quasi-streamwise vortex is almost uniform in the streamwise direction.
2. Temperature fields around the vortex for UHF and STG are also uniform in the streamwise direction. They are similar in shape, and they have azimuthal phase difference of about 90° since the mean temperature gradient for UHF and that for STG are in orthogonal directions.
3. Mean and fluctuation temperature has opposite gradient in wall-normal direction for UHF and in spanwise direction for STG. This inverted gradient is generated by the rotating motion of the vortex which transports excess temperature azimuthally around the vortex core.
4. Destruction process for wall-normal turbulent heat flux (in UHF) and that for spanwise components (in STG) are based on similar mechanisms. In both cases, destruction is caused by the rotating flow motion of the vortex, which results in low pressure within the vortex core and inverted gradient in temperature fluctuation near the vortex center-axis.

Acknowledgements

Author would like to express his thanks for the kind suggestion of data sampling method by Dr. H. Maekawa at the preliminary stage of the present work.

References

Black, A.W., Sparrow, E.M., 1967. Trans. ASME, J. Heat Transfer 89, 258–268.
Brooke, W., Hanratty, T.J., 1993. Phys. Fluids A 5 (4), 1011–1022.
Jeong, J., Hussain, F., Schoppa, W., Kim, J., 1997. J. Fluid Mech. 332, 185–214.
Kasagi, N., et al., 1992a. DNS database No. 02302043 supported by the Ministry of Education Science and Culture.
Kasagi, N., Tomita, Y., Kuroda, A., 1992b. Trans. ASME, J. Heat Transfer 114, 598–606.
Maekawa, H., Kawada, Y., Kobayashi, M., Yamaguchi, H., 1991. Int. J. Heat Mass Transfer 34 (8), 1991–1998.
Matsubara, K., Kobayashi, M., Maekawa, H., Suzuki, K., 1997. Trans. Jpn. Soc. Mech. Eng. 64 (619), 856–863.
Matsubara, K., Kobayashi, M., Maekawa, H., 1998. Int. J. Heat Mass Transfer 41, 3627–3634.
Miyake, Y., et al., 1995. Trans. Jpn. Soc. Mech. Eng. 61 (584), 1272–1278.
Quarmby, A., Quirk, R., 1972. Int. J. Heat Mass Transfer 15, 2309–2327.